Small-Angle Neutron Scattering by Highly Oriented Hybrid Bilayer Membranes Confined in Anisotropic Porous Alumina

Damien Marchal,*,† Christian Bourdillon,‡ and Bruno Demé§

Laboratoire d'Electrochimie Moléculaire, UMR 7591, Université Paris 7 Denis Diderot—CNRS, 75251 Paris, Cedex 05, France, Laboratoire de Technologie Enzymatique, UMR 6022, Université de Technologie de Compiègne, BP 20529, 60205 Compiègne, France, and Institut Laue-Langevin, BP 156, 38042 Grenoble Cedex 9, France

Received June 29, 2001. In Final Form: September 22, 2001

Small-angle neutron scattering (SANS) is used to characterize a phospholipid/alkoxysilane hybrid bilayer membrane (HBM), a model of biological membrane, supported in anisotropic porous alumina (Al_2O_3). The bilayer is obtained by fusion of phospholipid vesicles with a hydrophobic alkoxysilane monolayer chemically bound to the microporous alumina support. We first characterized the bare alumina material, then the alkoxysilane (OTS) layer bound to alumina, and finally the hybrid bilayer. By orienting the anisotropic support, we show that the intensity can be considerably increased, enabling the scattering to be measured in a wide q range ($6 \times 10^{-4} - 0.5$ Å^{-1}) corresponding to 9−10 decades in intensity and down to 10^{-4} cm^{-1}. This enables us to cover the structure factor of the oxide at large scale, the wide Porod regime, and the membrane form factor. Analysis of the scattering curves indicates that both the OTS layer and the HBM produce very smooth, uniform, and continuous layers at the alumina/solvent interface. This new approach in the characterization by SANS of a supported membrane in a porous material provides information on the homogeneity, the specific area, the roughness, and the thickness of the bilayer.

1. Introduction

Numerous models of biological membranes have been developed to enable the study of complex mechanisms occurring in natural membranes or at their interface. A consequence of the simplification need is that most investigated systems can be seen as rough models mimicking poorly the biological conditions. There is therefore a general attempt to make simple models of the membrane that specifically simulate the conditions of a reaction or the environment suitable for the stability of a given molecular structure. For instance, monolayers in the liquid state at an air−buffer interface are appropriate models for binding studies of soluble proteins and recognition processes at the buffer-lipid interface.[1] Other models such as HBM[2] (hybrid bilayer membranes) or bilayers supported at a solid-buffer interface[3] are adequate to mimic the lateral mobility of the components and have been also extensively studied. More recent studies have focused on bilayers having a higher degree of freedom, although they are still solid supported.[4] A higher lateral mobility can be achieved by several means such as the reduction of the number of binding sites to the support, the addition of a few flexible spacer molecules,[5] or the insertion of a soft polymer layer[6] to which the lipid membrane is loosely bound. In these conditions, the hydration and the dynamics of biological membranes are much better reproduced and the model becomes suitable, e.g., in studies of integral proteins with large soluble parts extending toward the aqueous phase. However, whatever the quality of the membrane model, it needs to be appropriate for the technique to be used which is itself determined by the information to be obtained.

In this context, most membrane models were developed to be suitable to characterization techniques which in most cases need a flat, smooth, and accessible surface. For instance, the presence of a bilayer can be detected by surface plasmon resonance (SPR) that measures immediate changes of the refractive index at the interface in proportion to the amount of material in the vicinity of the sensor surface.[7,8] Impedance analysis is based on the electric conductivity of the support. Using this technique, the quality of the membrane is evaluated by its capacitance which is related to the bilayer thickness and to the density of defects within the lipid bilayer.[9,10] Other techniques are used to control the homogeneity of the reconstituted bilayer like atomic force microscopy[11] or techniques using a fluorescent probe like fluorescence recovery after photobleaching (FRAP) to investigate the lateral diffusion of individual lipid molecules.[12] Fine studies were realized by neutron or X-ray reflectivity. These techniques are suitable to determine the scattering length density profile of the membrane with a good resolution.[13−15] From such information, it is possible to determine the thickness and

* To whom correspondence should be addressed. Damien Marchal, Laboratoire d'Electrochimie Moléculaire, UMR 7591, Université Paris 7 Denis Diderot—CNRS, 2 place Jussieu, T 44/55, 4e, case 7107, 75251 Paris Cedex 05, France. E-mail: marchal@paris7.jussieu.fr.

† Université Paris 7 Denis Diderot—CNRS.

‡ Université de Technologie de Compiègne.

§ Institut Laue-Langevin.

(1) Demé, B.; Hess, D.; Tristl, M.; Lee, L.-T.; Sackmann, E. *Eur. Phys. J. E* **2000**, *2*, 125.
(2) Plant, A. L. *Langmuir* **1999**, *15*, 5128.
(3) Tamm, L. K.; McConnell, H. M. *Biophys. J.* **1985**, *47*, 105.
(4) Sackmann, E. *Science* **1996**, *271*, 43.
(5) Lang, H.; Duschl, C.; Vogel, H. *Langmuir* **1994**, *10*, 197.
(6) Wagner, M. L.; Tamm, L. K. *Biophys. J.* **2000**, *79*, 1400.
(7) Cooper, M. A.; Try, A. C.; Carroll, J.; Ellar, D. J.; Williams, D. H. *Biochim. Biophys. Acta* **1998**, *1373*, 101.
(8) Lingler, S.; Rubinstein, I.; Knoll, W.; Offenhäusser, A. *Langmuir* **1997**, *13*, 7085.
(9) Gritsch, S.; Nollert, P.; Jähnig, F.; Sackmann, E. *Langmuir* **1998**, *14*, 3118.
(10) Steinema, C.; Janshoffa, A.; Ulricha, W. P.; Siebera, M.; Gallaa, H. J. *Biochim. Biophys. Acta* **1996**, *1279*, 169.
(11) Reviakine, I.; Brisson, A. *Langmuir* **2000**, *16*, 1806.
(12) Györvary, E.; Wetzer, B.; Sleytr, U. B.; Sinner, A.; Offenhäusser, A.; Knoll, W. *Langmuir* **1999**, *15*, 1337.
(13) Johnson, S. J.; Bayer, T. M.; McDermott, D. C.; Adam, G. W.; Rennie, A. R.; Thomas, R. K.; Sackmann, E. *Biophys. J.* **1991**, *59*, 289.

10.1021/la0110040 CCC: $20.00
Published on Web 11/27/2001

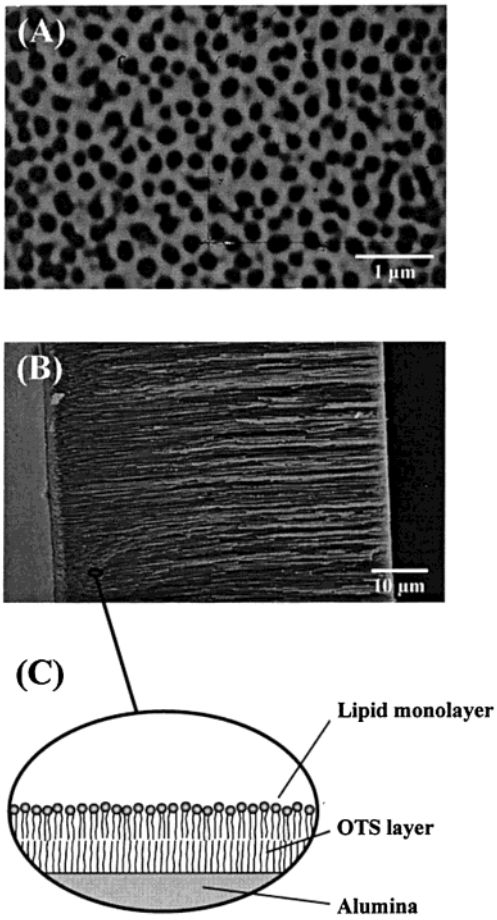

Figure 1. Front (A) and side view (B) of a 60 μm thick alumina membrane, and (C) detail of the inner surface of alumina bearing the HBM.

the compositional cross section of the membrane. Furthermore, these techniques are appropriate to study the interaction of different components with the membrane, providing for instance the location of membrane proteins[16] or bound polymer layers.[17,18]

In the present work, we have used small-angle neutron scattering (SANS) to characterize a HBM at the interface of porous aluminum oxide films (alumina; Figure 1) which cannot be investigated by the techniques mentioned above. It is the first step of a study aimed at investigating fully reconstituted phospholipid membranes loosely bound to their support which are more adequate models and that fulfill the conditions of an electrochemical detection via the coupling of the porous material to a gold electrode. The originality of the system results from the special geometry of the porous Al_2O_3 matrix that couples the HBM to the gold electrode. This artificial structure was designed to amplify electrochemical signals by increasing the reservoir of electrochemically active compounds localized in the bilayer. Studies of two-dimensional electron-transfer kinetics in the bilayer are made possible by the electrochemical control of the electron carrier pool (hydrophobic quinone) through its lateral mobility.[19] A preliminary characterization of the hybrid bilayer was realized in a previous study.[20] A stable dimyristoylphosphatidylcholine (DMPC) surface concentration of 250 ± 50 pmol cm^{-2} (66 Å^2) was measured by radiolabeling in the fluid bilayer, and the presence of a continuous supported membrane was demonstrated by measuring the diffusion coefficient of the electron carrier.[19]

SANS is a technique of choice that enables the study of this complex system, step by step, as the complexity of the self-assembly increases. This work is aimed at proposing a better description of the HBM model and to develop a new characterization technique of confined interfacial structures in a highly oriented anisotropic porous medium. SANS offers the unique potential to match alumina in an H_2O/D_2O mixture whose relatively high scattering length density yields an excellent contrast with protonated biological materials.

The method presented here is an alternative to reflectivity for studies of membranes confined in porous materials. We focus on the scattering by the interfacial films: the OTS layer chemically bound to the porous alumina and the supported lipid layer obtained after fusion with the vesicles. We show the potential of the SANS technique provided by the use of a regular matrix in a coaxial orientation of the pores relative to the beam axis that increases the scattering intensity by more than 1 order of magnitude compared to an equivalent but random interface.

Table 1. Molecular Weight, Density, Molecular Volume, and Scattering Length Densities of the Compounds Used in This Study[a]

compound		M, g mol^{-1}	*d*, g cm^{-3}	*V*, Å^3	$\rho \times 10^6$, Å^{-2}
water	H_2O	18	0.998	30	−0.56
heavy water	D_2O (99.9% D)	20	1.105	30	6.36
d-methanol	CD_3OD	36	0.890	67	5.83
octadecyl chain	$-C_{18}H_{37}$	253	0.777		−0.35
DMPC	$C_{36}H_{72}O_8NP$	677			0.34

[a] The scattering length densities are calculated from densities and scattering lengths, except for DMPC, whose scattering length density is from a contrast variation experiment.[40]

2. Materials and Methods

2.1. Reagents. 1,2-diacyl-*sn*-glycero-3-phospholcholine (DMPC, purity > 99%) was purchased by Avanti Polar Lipids (Alabaster, AL) and was used as received. Octadecyltrichlorosilane (OTS) was from Aldrich (Milwaukee, WI) and was distilled under vacuum before use. Hexadecane (Aldrich) was dried with desiccated molecular sieves. Aluminum oxides were commercial inorganic membrane filter disks (Anodisc 47 with a pore diameter of 200 nm) produced by Whatman (Maidstone, U.K.). Organic solvents were HPLC-grade. Water with a typical resistivity of 18 MΩ was produced by the Milli-Q purification system from Millipore (Bedford, MA). Heavy water (99.9% D) and deuterated methanol (CD_3OD, 99.8% D) were from Euriso-top (Saclay, France). Molecular weight, density, molecular volume, and scattering length densities of the compounds are given in Table 1.

2.2. Preparation of the Alumina and OTS Grafting. We used commercial Anodisc filtration membranes instead of those produced in our laboratory whose thickness (3 ± 0.5 μm) is too low for SANS experiments. Both are produced by anodization and can be used in the microporous electrode. Compared to our 3 μm thick membranes, Anodisc membranes (60 μm) represent a gain of a factor 20 of area in the beam. OTS grafting of the 60

(14) Meuse, C. W.; Krueger, S.; Majkrzak, C. F.; Dura, J. A.; Fu, J.; Connor, J. T.; Plant, A. L. *Biophys. J.* **1998**, *74*, 1388.
(15) Krueger, S.; Meuse, C. W.; Majkrzak, C. F.; Dura, J. A.; Berk, N. F.; Tarek, M.; Plant A. L. *Langmuir* **2001**, *17*, 511.
(16) Fragneto, G.; Graner, F.; Charitat, T.; Dubos, P.; Bellet Amalric, E. *Langmuir* **2000**, *10*, 4581.
(17) Majewski, J.; Kuhl, T. L.; Gerstenberg, M. C.; Israelachvili, J. N.; Smith G. S. *J. Phys. Chem. B* **1997**, *101*, 3122.
(18) Wong, J. Y.; Majewski, J.; Seitz, M.; Park, C. K.; Israelachvili, J. N.; Smith, G. S. *Biophys. J.* **1999**, *77*, 1445.
(19) Marchal, D.; Boireau, W.; Laval, J.-M.; Moiroux, J.; Bourdillon, C. *Biophys. J.* **1998**, *74*, 1937.
(20) Marchal, D.; Boireau, W.; Laval, J.-M.; Moiroux, J.; Bourdillon, C. *Biophys. J.* **1997**, *72*, 2679.

μm thick oxides was done by alkylation in a freshly prepared OTS solution in anhydrous hexadecane (0.5%, v/v) followed by 30 min of incubation. They were extensively rinsed in toluene by filtration afterward.

2.3. Supported Membranes. DMPC vesicles were prepared from the dry lipid as follows. A chloroform solution (13.5 mg) was evaporated under nitrogen flow and dried under vacuum for 1 h. The film was resuspended from the walls of a glass tube by vigorous vortexing in 20 mL of water. The solution was sonicated with a Branson 250 sonicator (Danbury, CT) set to a power of 60 W until turbidity had disappeared (4 times during 3 min). The temperature was maintained between 40 and 50 °C during sonication. Titanium particles were removed from the vesicle solution by a centrifugation at 3000 g during 10 min. Calibration of the vesicles' size was done by a further step of extrusion through 50 nm polycarbonate filters (25 times in an Avestin Lipofast Basic extrusion apparatus). The SUV solution (1 mM) was used during the day.

Fusion of the unilamellar vesicles with the inner OTS-treated surface of the microporous aluminum oxide was done according to the procedure described for alkylated glass coverslips by Brian and McConnell.[21] The microporous films were first wet with methanol and extensively rinsed with water. The support were then transferred and incubated in the solution of vesicles at 30 °C. Before use, the oxides were extensively rinsed with water for at least 1 h to eliminate freely suspended unfused vesicles.

2.4. Small-Angle Neutron Scattering. SANS experiments were performed on D11 and D22 at the high-flux reactor of the Institut Laue-Langevin, Grenoble, France. Four and three settings were used on D11 and D22, respectively, to cover a q range of 6×10^{-4}–6×10^{-1} Å^{-1}, i.e., 3 orders of magnitude in q. Data were corrected for the sample container scattering and instrument background and normalized to a water calibration run for detector efficiency corrections and scaling to absolute units (cm^{-1}). A flat background was subtracted to account for the incoherent scattering of the sample. For one of the samples, the diffractometer D16 was used to cover the wide-angle range with a better resolution.

2.5. Sample Holder and Orientation. The alumina sheets were oriented with their (macroscopic) surface normal to the neutron beam, thus, with the mean pore axis parallel to the beam axis (coaxial orientation). We used 1 mm thick circular quartz-QS windows from Hellma (Müllheim, Germany) with a diameter of 50 mm. These dimensions permitted us to use entire Anodiscs (diameter 37 mm, after the polypropylene ring had been removed) and a large circular diaphragm (16 mm) at the sample position. This also compensated the limited amount of illuminated material due to the membrane thickness (60 μm). The membrane was confined between the quartz windows, and the excess solvent was removed by pressing the windows against each other. By this way the membranes were perfectly wet and no residual solvent remained in the sample. Because alumina (Al_2O_3) has a very low incoherent scattering cross section (due to the low scattering length of Al and zero scattering of O), the residual incoherent signal resulted from the solvent (H_2O, D_2O, or CD_3OD) confined in the pores of the membrane and from the lipid film. For this reason, reducing the sample thickness to 60 μm was an important prerequisite to measure single layer form factors at the alumina–water interface and to reduce multiple scattering frequent at high contrast with porous materials exhibiting a high specific area. This made possible measurements of the scattering over 10 decades in intensity.

Using a highly ordered anisotropic support, it is crucial to adjust the orientation of the sample carefully. It is done by scanning it's vertical and horizontal rotations in a very low-q configuration where the hexagonal structure factor of the material is visible. At low q, the rocking curves go through a sharp maximum corresponding to the zero angle (coaxial orientation) where "boosting" of the signal is observed. To scan the vertical and horizontal rotations, we used a goniometer mounted on a rotation stage whose precisions are ± 0.01 degrees.

2.6. Analysis of Small-Angle Scattering Data. *2.6.1. Scattering by a Random Interface.* The scattering by a random interface defined by a steplike change of the scattering length density follows the Porod law:[22,23]

$$I(q) = 2\pi\Sigma\frac{1}{q^4}(\Delta\rho)^2 \tag{1}$$

where q is the scattering vector (Å^{-1}), Σ is the specific area of the sample (cm^2/cm^3), and $\Delta\rho$ is the contrast in scattering length density unit (Å^{-2}). In samples made of objects of well-defined shape, e.g., spheres, rods, etc., a dominating term related to the shape of the objects (the form factor) appears and the characteristic q^{-4} decay is only observed at high q where oscillations of the form factor vanish. This also holds for concentrated samples where a structure factor appears at low q for large objects. For this reason, useful information on the interface characteristics is extracted from Porod's law according to

$$\lim_{q\to\infty}[I(q)q^4] = 2\pi\Sigma(\Delta\rho)^2 \tag{2}$$

from which the specific area of the sample can be directly extracted given the contrast term. However, in principle, the Porod law can be observed in a wide range of intensities and scattering vectors as long as there are no scattering length density correlations in the sample due to defined shapes ($P(q)$) or interactions ($S(q)$) and as long as the orientation of the interface is random. If density correlations are present, it is observed only for $qd \gg 1$, where d is a characteristic correlation distance.

For interfaces whose roughness can be represented in real space by a Gaussian function, a Debye–Waller factor is used to account for the nonabrupt scattering length density profile of the interface. In this case, the scattering at wide angles decays much faster than q^{-4} and eq 1 becomes

$$I(q) = 2\pi\Sigma(\Delta\rho)^2\frac{1}{q^4}e^{-\sigma^2q^2} \tag{3}$$

where σ is the root-mean-square of the interface Gaussian distribution function centered on the average position of the interface.

2.6.2. Scattering by a Freely Suspended Membrane. The scattering produced by dilute "infinite" flat objects of finite thickness $2t$ and uniform scattering length density is given by[22]

$$I(q) = 4\pi\Sigma(t\Delta\rho)^2\frac{1}{q^2}\left(\frac{\sin qt}{qt}\right)^2 e^{-\sigma^2q^2} \tag{4}$$

In the case of membranes made of synthetic surfactants or phospholipids, it is common to distinguish the chain and head scattering length densities and thicknesses:[24]

$$I(q) = 4\pi\Sigma\frac{1}{q^2}\left(t_1\Delta\rho_{1,2}\frac{\sin qt}{qt} + t_2\Delta\rho_{2,3}\frac{\sin qt_2}{qt_2}\right)^2 \tag{5}$$

where t_1 and t_2 are the half thicknesses of the hydrophobic core and of the full membrane, respectively. $\Delta\rho_{1,2}$ and $\Delta\rho_{2,3}$ are the core–head and head–solvent contrasts.

2.6.3. Scattering by a Film at an Interface. Expressions of the scattering have been given for chemically grafted polymer layers producing dense brushes.[25] These relations can be simplified to the case of an interfacial layer having a uniform scattering length density in the normal and parallel directions to the interface, i.e., homogeneous in the plane of the interface and represented by a step function in the normal direction. The scattering function $I(q)$ becomes the sum of the interface and film contributions, plus a cross term:[26]

(21) Brian, A. A.; McConnell, H. M. *Proc. Natl. Acad. Sci. U.S.A.* **1984**, *81*, 6159.

(22) Porod, G. In *Small Angle Scattering*; Glatter, O., Kratky, O., Eds.; Academic Press: New York, 1982.

(23) Porod, G. *Koll. Z.* **1951**, *124*, 82

(24) Cantù, L.; Corti, M.; Del Favero, E.; Dubois, M.; Zemb, Th. *J. Phys. Chem. B* **1998**, *102*, 5737.

(25) Auvray, L.; Cotton, J.-P. *Macromolecules* **1987**, *20*, 202.

(26) Auroy, P.; Auvray, L.; Léger, L. *Macromolecules* **1991**, *24*, 2523

$$I(q) = \left[2\pi\Sigma(\Delta\rho_{1,3})^2\frac{1}{q^4} + 2\pi\Sigma(\Delta\rho_{2,3})^2\frac{1}{q^4}(1 - \cos q2t) - 4\pi\Sigma(\Delta\rho_{1,3})(\Delta\rho_{2,3})\frac{1}{q^4} + (1 - \cos q2t)\right]e^{-\sigma^2q^2} \quad (6)$$

where $\Delta\rho_{1,3} = \rho_1 - \rho_3$ is the solid−solvent contrast, $\Delta\rho_{1,2} = \rho_1 - \rho_2$ is the solid−film contrast, and $\Delta\rho_{2,3} = \rho_2 - \rho_3$ is the film−solvent contrast. Compared to grafted layers of soluble polymer chains, one can consider here that no water penetrates the layer of aliphatic chains, which means a volume fraction of chains $\phi = 1$ in the layer. In the particular case where the two sides of the film are matched to one another, $\Delta\rho_{1,3} = 0$ and the Porod and cross terms vanish. Equation 6 then simplifies to the scattering of a freely suspended film:

$$I(q) = \left[2\pi\Sigma(\Delta\rho_{2,3})^2\frac{1}{q^4}(1 - \cos q2t)\right]e^{-\sigma^2q^2} \quad (7)$$

which is equivalent to eq 4 with $1 - \cos q^2t = 2 \sin^2 qt$.

Equation 6 is valid when in-plane fluctuations of the scattering length density can be neglected, i.e., in the case of full coverage of the solid by a uniform layer. It is not valid in the case of a partial coverage or if defects are present (holes and inhomogeneities). Here, Σ accounts both for the specific area of the solid−liquid interface and that of the film−liquid interface which are supposed to be identical because of the dense and regular grafting of alumina by OTS.[27] The same argument supports the use of a single roughness parameter in Equation 6.

2.7. Fitting Procedures. To reduce the number of free parameters adjusted during a fit, the scattering length density of alumina was fixed to the value obtained by an independent contrast variation experiment (Figure 2). The scattering length densities of D_2O and water matched to alumina were fixed as well. We also proceeded step by step, starting from bare alumina where the fitted parameters were the specific area and the roughness, then with OTS where these parameters were fixed, and finally with the bilayer.

The scattering intensity being measured over several decades of intensity (9−10), fitting to the data was applied to $\log[I(q)]$ instead of $I(q)$ to give wide angle data the same weight as low angle ones to the calculation of χ^2. To further improve the procedure, only the intermediate to high q range was used to avoid the small angle region where the oscillations of $S(q)$ of the alumina structure modify the power law decay. Finally, experimental data being scaled to absolute units (cm^{-1}) and a flat background having been subtracted, no extra adjustable parameter was used to scale the fits, nor a background parameter used. Fitted parameters were directly adjusted from the analytical models calculated in absolute intensity and convoluted to the instrumental resolution.[28]

3. Results

3.1. Scattering by Pure Alumina Membranes. The scattering length density of alumina was measured by solvent contrast variation using D_2O volume fractions $\Phi(D_2O)$ ranging from 1 to 0.4. A plot of $I^{1/2}$ vs $\Phi(D_2O)$ is shown in Figure 2. A linear fit to the data yields the zero contrast point for a volume fraction of 0.731 corresponding to a scattering length density $\rho_1 = 4.50 \times 10^{-6}$ Å^{-2}. This is close to the value reported recently for bulk alumina.[29] However, this is significantly below the value expected for crystalline alumina if one considers the scattering length of Al_2O_3 and its density. Using a density of 1.25 g/cm^3 for the Anodisc 200 nm and a porosity of 39%,[30] we find a density of 3.2 g/cm^3 for bulk alumina. Assuming the Anodisc as being composed of pure Al_2O_3, these values

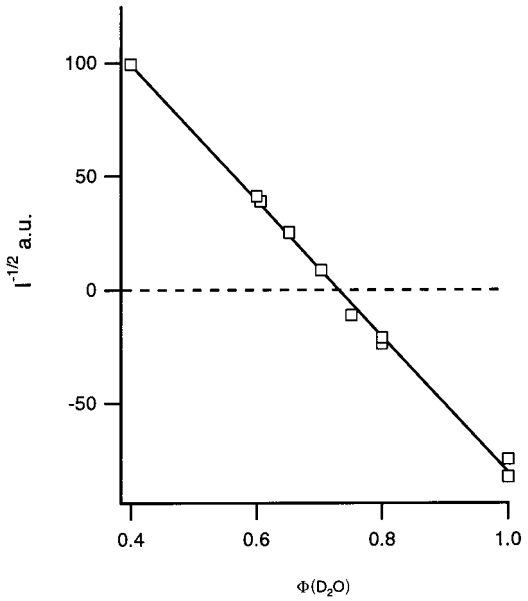

Figure 2. Determination of the alumina contrast match point by solvent contrast variation using H_2O/D_2O mixtures.

lead to a scattering length density $\rho_1 = 4.6 \times 10^{-6}$ Å^{-2}. The difference between the experimental value and the calculation is mainly due to the uncertainty on the porosity determination or to the presence of impurities in the alumina, like the presence hydroxyl groups that reduce the scattering length density of the material. Figure 3 shows the scattering of a 60 μm thick membrane-free alumina film wet by pure D_2O and measured in the coaxial orientation. In this configuration, the scattering curves are not sensitive to the longitudinal term of the cylinder form factor[31] but should be sensitive to the radial term (a Bessel function) related to the circular shape of the cylinder section. The pore walls are oriented in a grazing incidence (if not exactly coaxial) relative to the neutron beam. The very low q signal is due to the large scale in-plane distribution of holes which has a 2D-pseudohexagonal structure (honeycomblike), characterized by the 1, $\sqrt{3}$, $\sqrt{4}$, etc. sequence of pseudo-Bragg peaks.[32]

On Figure 3, no oscillations resulting from the radial term of the cylinder form are visible and a characteristic q^{-4} decay follows the hexagonal structure factor. It extends to the wide angle region, indicating a perfectly smooth interface. The solid line is a fit to the data according to eq 3 in the exceptionally wide Porod regime observed for this material. The fitted parameters are the specific area of the sample Σ and the roughness, with the contrast being known. The result of the fit to the scattering curve in Figure 3 is reported in Table 2.

At high q, the intensity is very sensitive to the local roughness of the material. The fit to the data according to eq 3 yields a roughness of 2 Å. Thus, the support can be considered perfectly smooth. To illustrate how the scattering is sensitive to the roughness parameter in the wide angle region, we show a simulation calculated with the same parameters but a roughness of 5 Å. The simulation yields an intensity 1 order of magnitude below the experimental intensity at $q = 0.3$ Å^{-1}.

3.2. Scattering by the OTS Layer. After silanisation, alumina becomes highly hydrophobic, and it is no longer possible to wet the surface with water. To measure the

(27) Sagiv, J. *J. Am. Chem. Soc.* **1980**, *102*, 92.
(28) Grillo, I. *ILL Technical Report* **2001**, *ILL01GR03T*, 20.
(29) Stefanopoulos, K. L.; Romanos, G. E.; Mitropoulos, A. C.; Kanellopoulos, N. K.; Heenan, R. K. *J. Membr. Sci.* **1999**, *153*, 1.
(30) Crawford, G. P.; Steele, L. M.; Ondris-Crawford, R.; Iannacchione, G. S.; Yearger, C. J.; Doane, J. W.; Finotello, D. *J. Chem. Phys.* **1992**, *96*, 7788.
(31) Pépy, G.; Kuklin, A. *Nucl. Instrum. Methods Phys. Res., Sect. B*, in press.
(32) Oster, G.; Riley, D. P. *Acta Crystallogr.* **1952**, *5*, 272.

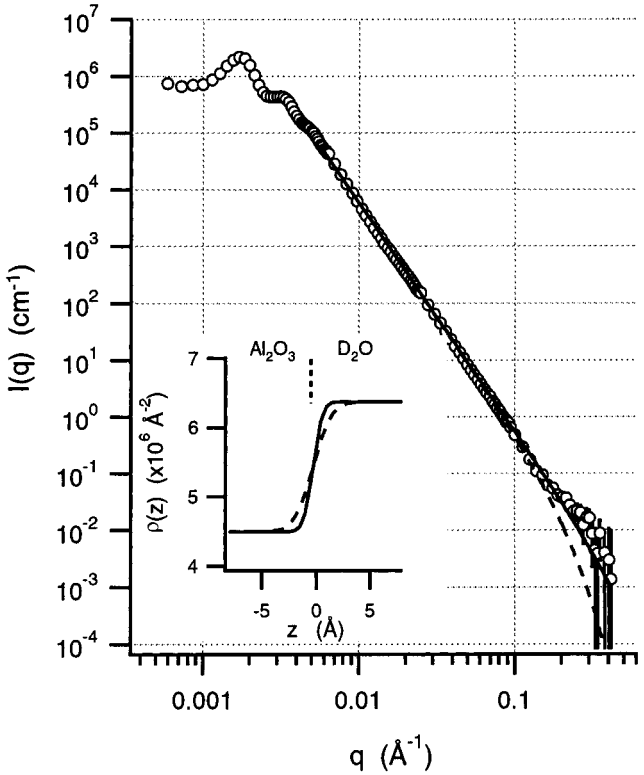

Figure 3. Small-angle neutron scattering of the membrane-free alumina support. Bragg peaks at very low q correspond to the pseudohexagonal (honeycomblike) pore distribution yielding an average center-to-center distance of 365 nm. The q^{-4} decay of the intensity results from the sharp alumina/water interface (nearly zero roughness). The solid line is a fit to the data according to eq 3. The dashed line is a simulation using the same alumina−D_2O contrast, the fitted specific area of the material, but a roughness of 5 Å. The insert represents the corresponding scattering length density profiles.

Table 2. Parameters Resulting from the Fit to the Data for the Three Systems Investigated[a]

	alumina	alumina−OTS	alumina−OTS−DMPC
solvent	D_2O	CD_3OD	H_2O/D_2O (26.9/73.1 v/v)
Σ, m^2/cm^3	433 ± 35	426 ± 34	433 ± 35
$\rho_1 \times 10^6$, Å^{-2}	4.50 ± 0.02	4.50 ± 0.02	4.50 ± 0.02
$\rho_3 \times 10^6$, Å^{-2}	6.36 ± 0.01	5.8 ± 0.02	4.50 ± 0.02
σ, Å	<2	2 ± 0.5	5 ± 1
$2t$, Å		25 ± 1	47 ± 5
$\rho_2 \times 10^6$, Å^{-2}		−0.3 ± 0.1	−0.4 ± 0.3

[a] Underlined parameters correspond to those who were fixed in the fitting procedure, whereas the others were adjusted. The scattering length density of alumina was always fixed because it was determined with an excellent precision by an independent contrast variation experiment. Only in the case of the OTS layer, all other parameter could be reliably adjusted because the film form factor and interface contribution to the scattering could be extracted from different part (q ranges) of the scattering curve. For the HBM (OTS−DMPC), the scattering length density of the hydrophobic layer had to be fixed to the fitted value obtained with OTS (and very close to the predicted value) because at the contrast match point of alumina the curve can be both adjusted by playing with Σ or ρ_2 given ρ_1.

OTS scattering, it is necessary to wet the hydrophobized oxides with an organic solvent like methanol. We have used fully deuterated methanol (CD_3OD) which produces a high contrast, instead of the CH_3OH/CD_3OD mixture that matches the scattering length density of alumina (4.50×10^{-6} Å^{-2}). Figure 4 shows the scattering of the

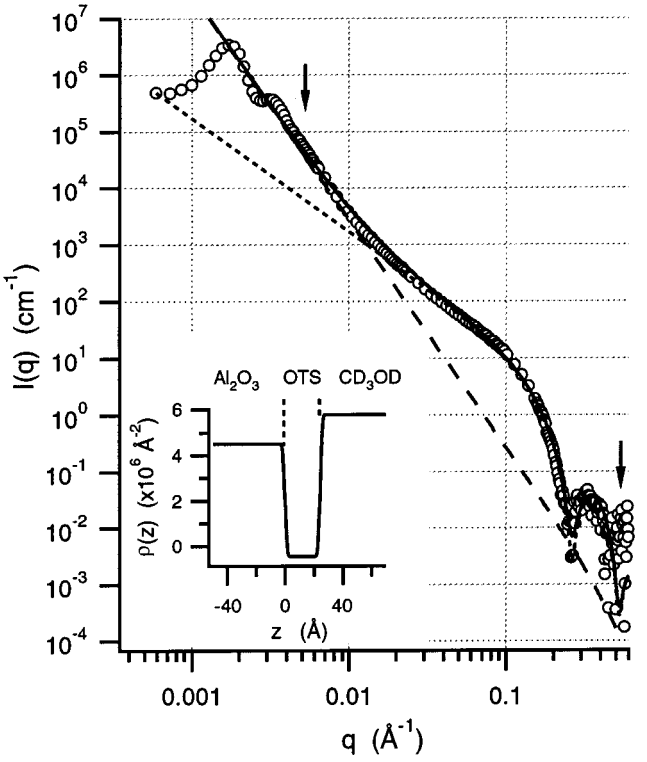

Figure 4. Small-angle neutron scattering by OTS grafted alumina wet by deuterated methanol (CD_3OD). Here, the contrast is such that the intensity results both from the interface scattering characterized by a q^{-4} regime and the film scattering characterized by a q^{-2} regime. Because of its much steeper decay, the q^{-4} is seen at low angles, whereas at higher q, the membrane scattering dominates (q^{-2} followed by oscillations). The best fit to the data according to eq 7 (solid line) yields a layer thickness of 25 Å and a roughness of 2 Å. The dashed and doted lines correspond to the interface and film contributions, respectively, whose sum plus a cross term yields the fit. The arrows indicate the q range taken into account for the fit. The insert represents the corresponding density profile.

OTS-grafted alumina at that contrast. Here, because alumina is not matched to the solvent, the intensity is the sum of the interface scattering (q^{-4} decay of Porod's law), the film scattering (q^{-2} decay), and of the cross term (q^{-4}; eq 6). Because the interface scattering decays much steeper than the film scattering, the later is observed at wide angles, whereas the interface scattering dominates at low angles. The part of the curve where the interface scattering dominates is used to adjust Σ and the scattering length densities of the OTS layer and of the solvent. The solid line in Figure 4 is the best fit to the data using eq 6 in the q range indicated by the arrows. In this q range, oscillations of the alumina structure factor have already vanished. The fit (Table 2) yields a film thickness $2t = 25$ Å, a roughness $\sigma = 2$ Å, and a scattering length density $\rho_2 = -0.3 \times 10^{-6}$ Å^{-2}. Like previously for the bare support, we fix the scattering length density of alumina to the value obtained by contrast variation ($\rho_1 = 4.50 \times 10^{-6}$ Å^{-2}). The corresponding scattering length density profile is shown in the insert. The dashed and dotted lines are the contributions of the interface and film scattering, respectively.

3.3. Scattering by the Hybrid OTS−DMPC Layer. After fusion of the vesicles with the OTS modified alumina, the interface is highly hydrophilic again and the pores can be wet by water. We have measured the scattering of the OTS−DMPC membrane with the H_2O/D_2O mixture (26.9/73.1 v/v) that matches alumina ($\rho_1 = 4.50 \times 10^{-6}$

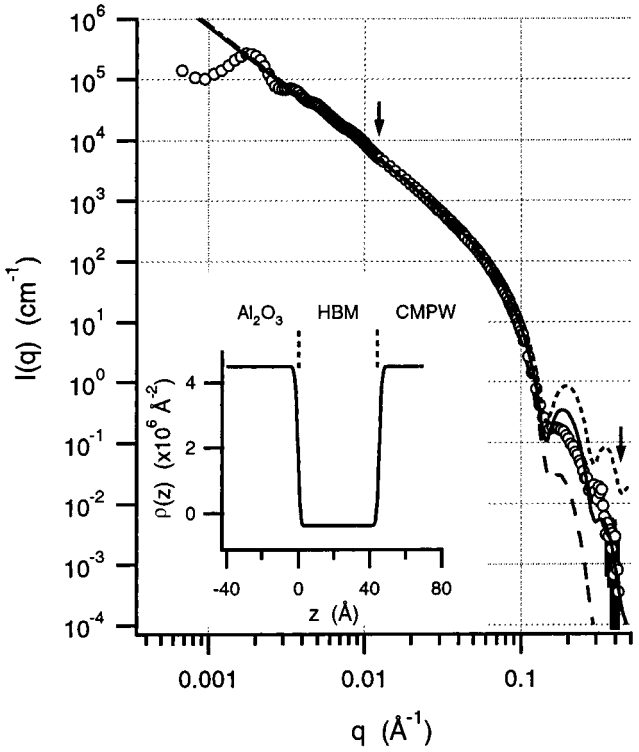

Figure 5. Small-angle neutron scattering of the hybrid bilayer supported by alumina matched to water (CMP). The contrast is such that the intensity only results from the membrane scattering "seen" as freely suspended and characterized by the wide q^{-2} regime. The best fit to the data according to eq 4 (solid line) yields a membrane thickness of 47 Å and a roughness of 5 Å. The arrows indicate the q range taken into account for the fit. The insert represents the corresponding density profile. The doted and dashed lines are simulations using a roughness of 0 and 10 Å, respectively.

Å^{-2}). The scattering of the hybrid bilayer is shown Figure 5. It is characterized by the expected q^{-2} decay and oscillations of the membrane form factor at wide angles. At that contrast, the bilayer is "seen" as a freely suspended film of finite thickness. In this case, eq 6 simplifies to eq 4 (or 7). Equation 5 cannot be used here to account for the polar head layer because of the asymmetry of the hybrid bilayer. The solid line in Figure 5 is a fit to the data using eq 4. It yields the membrane thickness (47 Å) and the membrane roughness (5 Å). A fit to the data using eq 6 where the solvent scattering length density ρ_3 is left free yields an alumina-solvent contrast of the order of 10^{-8} Å^{-2} indicating that the q^{-4} interface scattering is negligible, i.e., that the solid support is perfectly matched to the solvent.

4. Discussion

The main difference from a classical specular reflectivity experiment (among others such as resolution) results from the orientation of the reflecting surface which is not singular here but have the same probability for all parallel orientations of the interface relative to the beam, with some spread around the mean orientation of the pores due to irregularities. In the coaxial configuration, the first consequence is that the scattering remains isotropic although the interface is highly oriented. The second one is that radially averaged data yield an ideal Porod behavior with a characteristic q^{-4} decay of the intensity. We observed a tolerance of ca. $\pm$ 1° around $\phi = 0$ where the scattering remains isotropic, and we can conclude that this angular window of 2° is related to the spread in the pore orientation around the mean value set to zero in these experiments.

Validity of the Porod Law. In the coaxial configuration used here, with pores of cylindrical shape oriented parallel to the incident beam, we are very close to reflectivity conditions. Our analysis is based on the fact that Porod's law results from the reflection of the incident neutrons on portions of the interface which have the right orientation to yield a reflection at a given scattering angle.[33] Using 4.5 Å neutrons and alumina in D_2O, total reflection occurs for any angle θ below $\theta_c = 0.2°$, but reflection events can also take place for $\theta > \theta_c$ with $R(\theta) < 1$ and following a q^{-4} decay according to Fresnel's law. By orienting a highly anisotropic interface so that the probability to have a reflection is increased, it is possible to boost the scattering intensity. In this case, the q^{-4} decay of the intensity is kept but the coefficient $2\pi\Sigma(\Delta\rho)^2$ is modified, and thus, the measured Σ is only apparent. The remaining question is whether the q^{-4} decay is sufficient to claim that Porod's law and analytical models of the interface structure are valid. The q^{-4} decay characteristic of Porod's law has already been shown to hold for this type of material in the case of Anodisc 20 nm membranes,[34] but the authors did not measure the low q region and claimed that scattering was much better explained by assuming a random pore structure. We think that despite some irregularities in shape and size of the pores the dominating feature of the material is its anisotropy.

Because of this strong anisotropy, isotropic scattering is only observed when the orientation of the sample is correctly adjusted. Rotating the sample apart from the coaxial orientation ($\phi = 0$) yields highly anisotropic patterns in the very low q region where the hexagonal structure factor of the material is visible. In the Porod regime, the intensity decreases when the sample angle increases, because the probability for a reflection to take place at the interface decays with the angle between the pores and the incident beam. This is also combined to the increase of anisotropy at low q.

Specific Area and Roughness. The specific area of alumina is evaluated according to eq 3. If one refers to the known specific area of Anodisc 200 nm membranes (7.7 m^2/cm^3),[30] the "boosting effect" is considerable: a gain of a factor of ca. 50 results from the coaxial orientation of the interface (see Table 2). Specific areas extracted in this configuration are thus apparent because the proportion of interface yielding a reflection and contributing to the q^{-4} law is artificially increased compared to a random interface (e.g., like in suspensions of spheres, vesicles, randomly oriented rods, etc.).

The roughness of the bare alumina support is extremely low (2 Å, Figure 3), which makes porous alumina suitable for the study of thin supported films whose scattering is observed at high q. A rough support would lead to a much faster decay of the scattering than the q^{-4} decay observed here and would make the intensity much more difficult to measure.

With the OTS-grafted alumina, in the intermediate to high q range, the intensity decay turns from the q^{-4} decay of bare alumina into a q^{-2} dependence followed by oscillations characteristic of a thin film. We can see from Figure 4 and Table 2 that the best contrast yielding an independent determination of the apparent specific area and film scattering length density is the one that yields

(33) Auvray, L.; Auroy, P. In *Neutron, X-ray and light scattering*; Zemb, Th., Ed.; North-Holland: Amsterdam, 1991; p 199.

(34) Su, T. J.; Lu, J. R.; Cui, Z. F.; Thomas, R. K.; Heenan, R. K. *Langmuir* **1998**, *14*, 5517.

two characteristic behaviors in distinct q ranges, highlighting the interface at low q (Σ, $\Delta\rho_{1,3}$) and the film at high q (thickness, roughness, density ρ_2). As seen in Figure 4 the interface scattering leads to very high intensities that dominate the film scattering at low q. In this q range, an accurate determination of the apparent specific area of the sample is possible given the scattering length density of the solid support. In our case, the scattering length density of porous alumina is known from the contrast variation experiment (Figure 2), and we only fit the apparent specific area of the sample in this q range.

Exposure of the polar metal oxide surface to OTS solutions results in a covalent binding of the silane molecules to the oxide surface.[27] The lateral formation of the siloxane bridges and weak dispersive interactions between hydrocarbon chains result in monolayers of nearly perfectly packed chains. The high chain density was evidenced by Gun and Sagiv by infrared spectroscopic and contact angle measurements.[35] We have used the same immobilization procedure to attach the monolayer of OTS to the internal surface of porous aluminum oxide films. Well resolved oscillations of the OTS form factor are due to the constant thickness of the layer and to the sharpness of the interface. The roughness of 2 Å shows self-consistently that eq 6 is valid when both the alumina and the film contribute to the scattering. Effectively, the roughness being the same for bare alumina and for the film surface, a single roughness parameter can be used. Furthermore, a rough film (due to local out-of-plane fluctuations or defects) bound to a sharp interface would lead to a scattering dominated by the q^{-4} alumina contribution, whereas the film scattering would decay much faster at high q. In the range of roughnesses observed here, it is still possible to measure the oscillations and to have a good precision on the roughness. The same value found for the support and the film is also consistent with the way the OTS layer is produced with a postreticulation of Si groups in the first plane of atoms bound to the alumina that reinforces the regularity of the layer.

Thickness and Density of the Layers. The thickness of the OTS layer is in good agreement with previously published data.[36,37] Compared to reflectivity studies,[37] the precision found by SANS is the same. The thickness measured for fluid DMPC membranes in the L_α phase is 42 Å.[13] We found a thickness equal to 47 ± 5 Å for the HBM. The scattering length density of the layer is close to the one expected for a pure layer of aliphatic chains (Table 1). Because of the single-layer model used to fit the data, the uncertainty in the determination of the thickness and of the roughness of the layer are slightly higher than in the case of OTS.

However, the presence of defects or islands (i.e., thickness or density fluctuations) in the layers can be discarded in the case of both OTS and HBM. For a structure containing islands, the position of the first minimum in the SANS profile would be the same as for a continuous homogeneous monolayer because the distance between the solvent−layer and layer−alumina interfaces would be the same. However, the intensity would change because the in-plane averaged scattering length density within the island-containing layer would be higher than that within the island-free monolayer. For a homogeneous layer with thickness fluctuations, the first minimum would be less sharp and its roughness would increase, but the measured thickness would be roughly the same. Furthermore, we only observed a slight increase from 2 Å for the OTS to 5 Å for the hybrid bilayer.

At the alumina contrast match point, eq 6 is valid because no scattering originates from the alumina surface whose roughness is different from the bilayer one. For any other contrast, this relation is not valid, and a model using two roughness parameters would be required. In the case of HBM studies at the alumina contrast match point, another argument is in favor of a defect-free layer (no islands): if the bilayer were containing water (due to holes or a slight solubility in the layer), this would change significantly the average scattering length density of the layer. For instance, a layer containing 5% of water at the CMP would yield a mean scattering length density of 0.035 $\times 10^{-6}$ Å^{-2}, instead of -0.4×10^{-6} Å^{-2} found experimentally.

So, careful data treatment in the wide angle regime allows us to measure the intensity down to 10^{-4} cm^{-1} (up to 0.5 Å^{-1} in reciprocal space) which makes a detailed analysis of the interface structure possible with a resolution of the order of 1−2 Å for a sensitive parameter like the roughness. In the case of the HBM, a more refined description of the interfacial layer could be obtained by using a model accounting for the layer of headgroups, i.e., the asymmetry of the hybrid bilayer, and by selective deuteration of either the OTS,[37] the DMPC aliphatic chains, or the headgroups.[38] The state of the aliphatic chains in each hemimembrane, solid or liquid crystalline, could be determined with deuterated acyl chains producing a wide angle signal characteristic of the chain packing. However, rather than refining the analysis of hybrid bilayer membranes, we wish to concentrate on assemblies which mimic biological membranes in order to investigate specific biological processes.[39]

5. Conclusion

Alumina films known as Anodisc membranes are appropriate supports in studies of confined interfacial structures by neutron scattering. Their scattering length density, high specific area, and nearly perfectly sharp internal surface make studies on very small amounts of material possible, and they are thus appropriate for biological studies at interfaces. Compared to a reflectivity experiment, a few square centimeters of porous alumina correspond to several square meters of interface in the beam. Furthermore, thanks to the possibilities of chemical derivatization, anisotropic porous alumina is a support of choice for a number of systems that were to now only investigated on flat, smooth and directly accessible surfaces (grafted or adsorbed polymer layers, supported membranes, self-assembled structures, etc.). The sharpness and the great specific area of this support make this material a standard support for interfacial studies by SANS like for instance silicon wafers in reflectivity studies.

In our case, investigation of the HBM in the confined medium was motivated by the in situ characterization of the model membrane. We use the "boosting effect" resulting from the coaxial orientation of the interface parallel to the beam to realize this study in the porous material. Analysis of the scattering curves gives substantial details on the interfacial layer with the determination of its thickness, roughness, and scattering length

(35) Gun, J.; Sagiv, J. *J. Colloid Interface Sci.* **1986**, *112*, 457.
(36) Wasserman, S. R.; Whitesides, G. M.; Tidswell, I. M.; Ocko, B. M.; Pershan, P. S.; Axe, J. D. *J. Am. Chem. Soc.* **1989**, *111*, 5852.
(37) Fragneto, G.; Lu, J. R.; McDermot, D. C.; Thomas, R. K.; Rennie, A. R.; Gallagher, P. D.; Satija, S. K. *Langmuir* **1996**, *12*, 477.
(38) Majkrzak, C. F.; Berk, N. F.; Krueger, S.; Dura, J. A.; Tarek, M.; Tobias, D.; Silin, V.; Meuse, C. W.; Woodward, J.; Plant, A. L. *Biophys J.* **2000**, *79*, 3330.
(39) Marchal, D.; Pantigny, J.; Laval, J.-M.; Moiroux, J.; Bourdillon, C. *Biochemistry* **2001**, *40*, 1248
(40) Demé, B.; Zemb, Th. *J. Appl. Crystallogr.* **2000**, *33*, 569.

density. The results indicate that both the OTS layer and the HBM produce very smooth, uniform, and continuous layers at the alumina/solvent interface.

We also come to the conclusion that these supports need to be very carefully oriented because of the strong angular dependence of the scattering intensity and the strong anisotropy that appears apart from the coaxial orientation of the pores relative to the beam axis. In this respect, it is necessary to have access to the very low q range where anisotropy is best observed, although useful information on the interface structure is observed at much higher q. A finer analysis model is in development to integrate the honeycomb structure of the material (the cylinder structure factor) and the pore (cylinder) form factor at any angle apart from the coaxial configuration.

Acknowledgment. The authors are grateful to L. Auvray for critical reading of the manuscript and to G. Pépy for stimulating discussions and sharing of his unpublished results.

LA0110040